Bulgarian Chemical Communications, Volume 55, Issue 3 (pp. 183-187) 2023 *DOI: 10.34049/bcc.55.3.5498*

Hydrogen sorption and electrochemical hydriding of $Mg_{2.1}Ni_{0.7}V_{0.3}$

E. Grigorova[1*], S. Todorova[2], P. Tzvetkov[1], T. Spassov[2*]

[1]*Institute of General and Inorganic Chemistry, Bulgarian Academy of Sciences, Acad. G. Bonchev Str., Bl. 11, 1113 Sofia, Bulgaria*

[2]*Faculty of Chemistry and Pharmacy, Sofia University "St. Kliment Ohridski", 1 James Bourchier Blvd., 1164 Sofia, Bulgaria*

Received: June 07, 2022; Revised: June 10, 2023

Mixture of metals with overall composition corresponding to $Mg_{2.1}Ni_{0.7}V_{0.3}$ is prepared by ball milling under Ar atmosphere. Hydrogen sorption characteristics of the mixture are determined at different temperatures in a volumetric Sievert-type apparatus. Hydrogenation at 300^0C and 1MPa results in 3.8 wt. % H_2 absorption capacity with improved hydriding kinetics, explained by the refined particle size attained by appropriate milling. Hydrogen desorption at 300^0C and 0.15 MPa is found to proceed with high rate as well. Slower, but still relatively fast desorption rate compared to this at 300^0C is registered at 280^0C. After hydriding, the sample is characterized by X-ray diffraction analysis and SEM, revealing the phase composition of the powder mixture- orthorhombic and monoclinic Mg_2NiH_4 as main phases and small amounts of MgH_2, Ni and VH_x. The electrochemical hydrogen charge/discharge behavior of this material is studied as well, but because of rapid corrosion the electrochemical capacity drops down after the first cycle only.

Keywords: hydrogen storage; Mg_2NiH_4 hydride; ball milling; NiMH battery

INTRODUCTION

A detailed review of magnesium-based alloys, compounds, and composites for hydrogen energy storage is published by Yartys *et al.*, with a conclusion that they can be very attractive not only as solid-state hydrogen storage media but also for storage of concentrated solar heat and in the future as novel type magnesium batteries replacing lithium ones [1]. One of these promising materials is the intermetallic Mg_2Ni, forming Mg_2NiH_4 hydride with improved hydriding kinetics in comparison to Mg and theoretical hydrogen storage capacity of 3.6 wt. %. Mg_2NiH_4 has some interesting properties related to its polymorphs – different color, structure, and electric properties. Some authors as Gavra *et al.* [2], Rönnebro *et al.* [3], Li *et al.* [4], Cermak *et al.* [5, 6], Orimo *et al.* [7], Varin *et al.* [8, 9] and other [10-17] carried out studies on the formation and decomposition of this hydride. The polymorphs of Mg_2NiH_4 are two low-temperature phases – monoclinic with metal-like electrical conductivity and orthorhombic crystal structures with orange-rust color and insulator properties and a high-temperature one with a cubic structure [4, 5]. For the synthesis of Mg_2NiH_4 different methods are applied as combustion synthesis [4] or ball milling of Mg and Ni and hydrogenation [5], or reactive ball milling under hydrogen of MgH_2 and Ni [6, 9, 13]. A review on different intermetallic compounds including Mg_2Ni and its hydrides, prepared by mechanical alloying is published recently by Liu *et al.* [18].

The Mg_2Ni-type intermetallics have shown potential as an anode material in Ni-MH batteries as well. The development of high capacity and low-cost anode material is of great importance for the extensive production and application of these batteries. The theoretical electrochemical capacity of Mg_2Ni is reported to be close to 1000 mAh/g. However, the electrochemical cycle characteristics of Mg-based materials fail to meet the requirements for practical application, because they are easily oxidized in alkaline solution electrolyte used in the battery leading to much lower experimental discharging capacities than the theoretical ones [19-25]. Some authors proved that partial substitution of Ni in Mg_2Ni by La or Cu and melt-spinning as a preparation technique improve the electrochemical characteristics [22, 23].

Main subject of the present work is the synthesis of the ternary hydride Mg_2NiH_4 applying an easier and faster approach at lower temperature and pressure and optimized ball milling conditions compared to previously reported [12-14]. Both, gas-solid hydrogen absorption-desorption properties at different temperatures and electrochemical charge/discharge behavior of the prepared material were studied. In general, this study extended our recently published results on $Mg_{2.1}Ni_{0.7}V_{0.3}$

* To whom all correspondence should be sent:
E-mail: egeorg@svr.igic.bas.bg;
tspassov@chem.uni-sofia.bg

hydriding [26]. The novelties in the present work are the extended ball milling time with the aim to obtain a more active material with increased number of defects and level of amorphization and to investigate the hydrogen sorption properties in gas phase and electrochemically in the absence of carbon additive.

EXPERIMENTAL

Ni powder sized less than 150 μm with a 99.99% purity and V powder 325 mesh with a 99.5% purity purchased from Sigma Aldrich (Munich, Germany) were used for the preparation of the mixture. Mg powders with purity 99% and 50 mesh were purchased from Strem Chemicals (Newburyport, MA, USA). $Mg_{2.1}Ni_{0.7}V_{0.3}$ composite was synthesized by ball milling under Ar atmosphere, followed by annealing in hydrogen atmosphere. High-purity argon (99.999%) and hydrogen (99.99%) purchased from Messer were used for the experiments. The mixture was ball milled under argon in a planetary mono mill Pulverisette 6 Fritsch (Thuringia, Germany) using the following conditions: ball-to-sample weight ratio of 10:1, stainless steel balls with diameter of 10 mm, vial volume of 80 cm^3, rotation speed of 200 rpm and duration of 6 and 10 h. After 6 and 10 h of ball milling, the vial was opened in a glove box under argon and a small portion was taken for X-ray diffraction analysis. Also, the powder was manually removed from the wall of the vial and the balls. Hydrogen absorption-desorption characteristics were studied at various temperatures using self-constructed Sievert type apparatus. After milling and hydrogenation, the sample was characterized by X-ray diffraction phase analysis using powder X-ray diffractometer Bruker D8 Advance with a LynxEye detector and Cu Kα radiation.

The electrochemical hydrogen charge/discharge of the composite was performed in a three-electrode cell and 6 mol/dm^3 KOH electrolyte, permitting accurate control of the electrodes' geometry. The working electrode with an area of 1 cm^2 and a thickness of about 2 mm was prepared by mixing 100 mg of the synthesized alloys with 70 mg of teflonized carbon, adding a few droplets of heptane. $NiO(OH)/Ni(OH)_2$ was used as the counter-electrode, and the reference electrode was Ag/AgCl. The charge (charge time of 4h) and discharge current densities were 50 mA/g and 20 mA/g, respectively, and the voltage to which the electrodes were discharged was 0.5 V. For the hydrogen diffusion coefficient determination two electrodes were prepared – the first one with gas phase hydrided alloy and the second one electrochemically hydrided after one charge/discharge cycle. Both were discharged under potentiostatic conditions at a potential of 0.6 V.

RESULTS AND DISCUSSION

Figure 1 presents X-ray diffraction patterns of a Mg-Ni-V mixture with a composition corresponding to the formula $Mg_{2.1}Ni_{0.7}V_{0.3}$ after two different ball milling times, as well as of a sample ball-milled (10 h) and then hydrogenated at 300^0C and 1 MPa. Even after ten hours of milling no newly formed phases were observed, but just the diffraction lines of unreacted Mg, Ni and V metals. Some very small increase of the background and the intensity of nickel diffraction lines could only be detected.

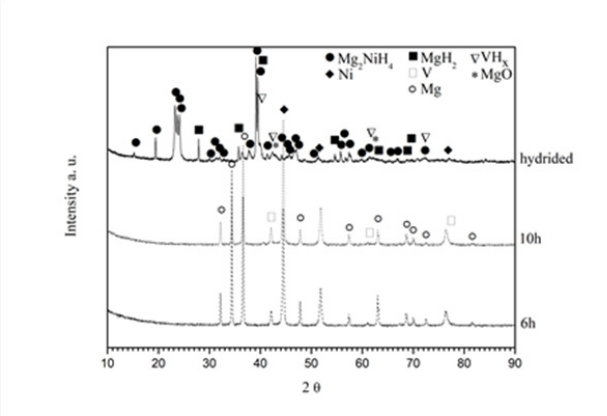

Figure 1. X-ray diffraction patterns of Mg-Ni-V mixture after 6 and 10 h of ball milling and of a sample ball milled (10 h) and then hydrided.

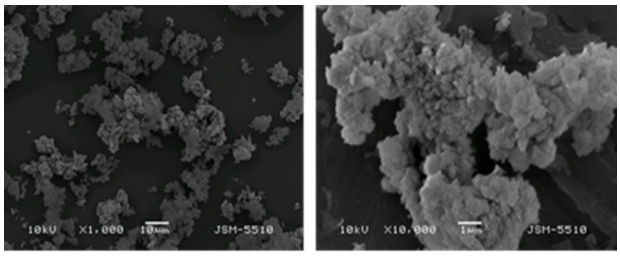

Figure 2. SEM micrograph of a Mg-Ni-V mixture, ball milled for 10 h and hydrided.

Milling for 10 h and hydriding produces fine metallic particles, the largest ones close to 1000 nm (Figure 2). Particles' agglomerations (soldering) are also observed due to the softness of the main metal (Mg) in the mixture. Obviously, the absence of anti-sticking agent in the composite, as for example activated carbon [26], leads to material agglomeration and sticking to the milling balls and walls.

During hydrogenation, the ball-milled composite transforms into Mg_2NiH_4 with monoclinic and orthorhombic polytypes as main phases, as well as VH_x and a small amount of unreacted Ni and MgH_2.

Comparison with previously published results by the authors [26] shows less visible X-ray diffraction lines of unreacted Ni, revealing that more complete transformation to Mg_2NiH_4 is achieved in the current study. A semiquantitative phase analysis for the composite $Mg_{2.1}Ni_{0.7}V_{0.3}$ was made by using DiffracPlus EVA program [27] and RIR (reference intensity ratio) method, showing: MgH_2 - 13%, Mg_2NiH_4 - 81%, VH_x - 2-3% and MgO - 2-3 %. Hydrogen absorption curves are presented in Figures 3 and 4. In Figure 3 hydrogen absorption curves of $Mg_{2.1}Ni_{0.7}V_{0.3}$ ball milled for 10 h with different hydrogenation cycles at 300^0C and 1 MPa are presented. It is shown that only after the first hydriding/dehydriding cycle the hydriding kinetics is noticeably improved. Almost complete hydriding was reached for less than 10 min and the absorption capacity was 3.3 wt. % H_2 after only 3 min of hydrogenation. This is a very promising result for this type of material. The maximum absorption capacity of 3.8 wt. % H_2 was measured for the composite after 7 cycles. It should also be mentioned that except for the first activation cycle, all other hydrogenation cycles showed similar hydrogen absorption kinetics and capacity (Figure 3). Similar hydrogen storage capacity value, 3.76 wt. % H_2 for $Mg_2Ni_{0.75}Cu_{0.25}$ at 300^0C, but at higher pressure of 2.8 MPa has been shown by M. V. Simicič *et al.* [25].

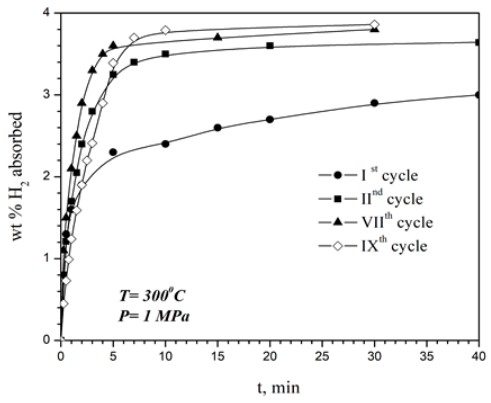

Figure 3. Hydrogen absorption curves of $Mg_{2.1}Ni_{0.7}V_{0.3}$ at different cycles.

In Figure 4 the hydrogen absorption curves at 300^0C and 200^0C for composites of the same type, but milled for a different time with and without activated carbon are compared. As it was mentioned in the Introduction part of this study, the ball milling duration is longer, e.g., 10 h with the idea to obtain more active material with introduction of an increased number of defects. Longer ball milling leads to particles' size refinement, more defects, better contacts between the metallic particles, and also larger fresh non-oxidized surface.

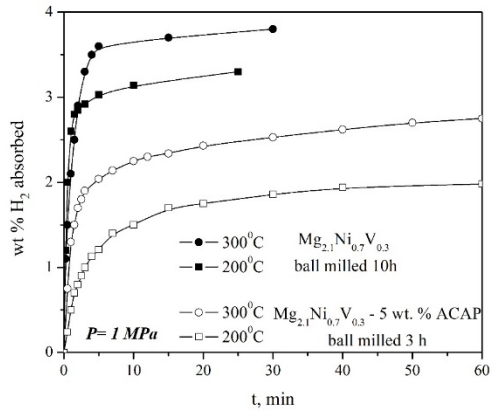

Figure 4a. Hydrogen absorption curves of $Mg_{2.1}Ni_{0.7}V_{0.3}$ and $Mg_{2.1}Ni_{0.7}V_{0.3}$ - 5 wt. % ACAP [26] at 300^0C and 200^0C.

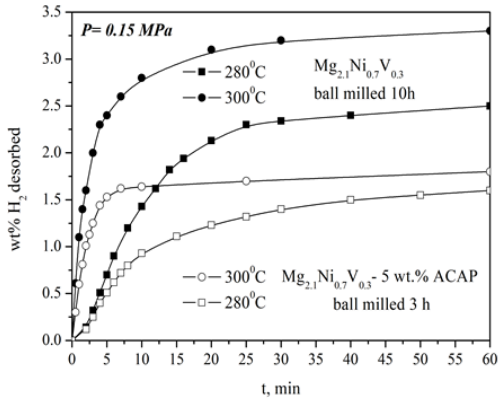

Figure 4b. Hydrogen desorption curves of $Mg_{2.1}Ni_{0.7}V_{0.3}$ and $Mg_{2.1}Ni_{0.7}V_{0.3}$ - 5 wt. % ACAP [26] at 300^0C and 280^0C.

All these effects cause improved absorption kinetics and increased hydrogen absorption capacity. After hydrogenation at 300^0C and 1 MPa of $Mg_{2.1}Ni_{0.7}V_{0.3}$ milled for 10 h under argon we could also confirm the change in the color of the composite (orange-rust reddish); an effect which other authors have also observed [2, 3].

The desorption curves at 300^0C and 280^0C for the two composites - the current one $Mg_{2.1}Ni_{0.7}V_{0.3}$ ball milled for 10 h and $Mg_{2.1}Ni_{0.7}V_{0.3}$ - 5 wt% ACAP ball milled for 3 h [26], are also compared, Figure 4b. Improved hydrogen desorption kinetics and increased desorption capacity was detected for $Mg_{2.1}Ni_{0.7}V_{0.3}$ ball milled for 10 h at both temperatures. Other authors have shown that Mg_2Ni-type materials with partial substitution of Ni by Cu

or V can desorb hydrogen at 200^0C, but under vacuum [25].

The hydrogen-sorption properties of the alloy were also electrochemically characterized.

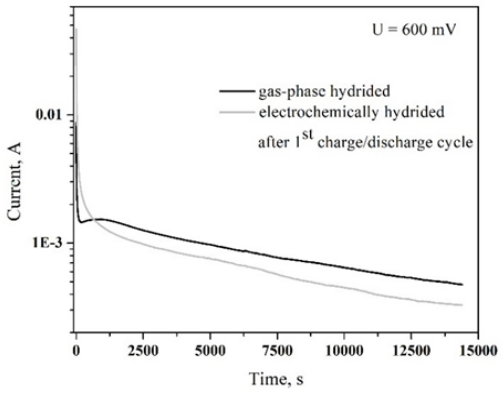

Figure 5. Charge-discharge curve (a) and cycle stability of $Mg_{2.1}Ni_{0.7}V_{0.3}$ ball milled for 10 h (b).

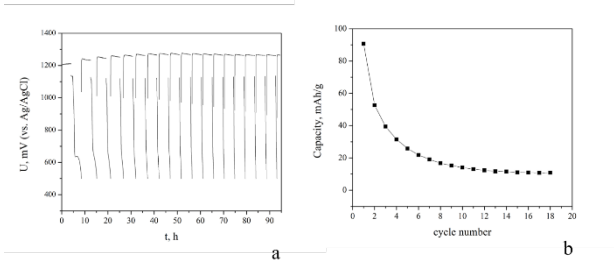

Figure 6. Current *vs*. time during H-discharge of the hydrided Mg_2Ni-based material.

Figure 5 shows hydrogen charge/discharge curves of the obtained composite, applying relatively low current densities of charge and discharge. In contrast to the very good hydrogen sorption characteristics of the composite from a hydrogen gas phase, at electrochemical hydrogenation the discharge capacity is low. Compared to the capacities of other similar Mg_2Ni based compositions our results are between measured lower or close [19, 20, 22, 32] and higher [20, 22 - 24, 25, 29, 31, 32] capacity values. The rapid reduction of the discharge capacity is clearly visible, which can be explained by the chemical corrosion of the alloy. An additional reason for the low corrosion stability of the alloy is its fine-particle nature formed during prolonged grinding at a sample-to-ball mass ratio of 1:10, as well as the high intensity of the grinding process.

In order to shed light on the factors determining the improved gas-phase hydriding kinetics, additional electrochemical experiments were performed to determine the diffusion coefficient of hydrogen in the alloy. Figure 6 shows a potentiostatic discharge of the fully gas-phase hydrided sample and of a sample electrochemically hydrided after one charge/discharge cycle. This analysis allows to obtain the diffusion coefficients of hydrogen, DH, calculated according to a methodology described by Zheng *et al.* [28]. Due to the difficulty of determining the average particle size (because of agglomeration), we can indicate here only the interval of the diffusion coefficient, 4.10^{-12} m^2/s - 4.10^{-10} m^2/s, taking particle diameters of 1 and 10 μm, respectively. DH values in the range of 4.10^{-11} m^2/s - 4.10^{-10} m^2/s are also reported by other authors for Mg_2Ni based materials [29-32].

It is well known that the hydrogen sorption characteristics of Mg_2Ni-based materials from a hydrogen gas phase surpass those obtained by electrochemical hydrogen for charge/discharge [24, 25], as the most probable reason is the higher sensitivity of these materials toward oxidation in alkaline water solutions. In agreement, it was already reported that longer ball milling could result in distributed electrocatalytic active sites, larger interface, smaller particle size, and higher reactivity due to higher defects density, but on the other hand, excessive milling damages the crystal lattice and causes a sharp drop in electrochemical capacity [20].

CONCLUSIONS

A mixture of metals with general composition $Mg_{2.1}Ni_{0.7}V_{0.3}$ was milled under an argon atmosphere at more energetic/intensive milling conditions and its hydriding properties were studied both in a hydrogen gas atmosphere and electrochemically. The capacity and kinetics of hydriding were found to be noticeably improved compared to a material with the same composition but milled with carbon additives. As expected, during electrochemical hydriding/dehydriding this alloy suffers from significant corrosion, which limits its hydrogen storage capacity and cycling stability. The present study shows that improved hydriding properties of the synthesized material are most probably a result of both the suitable combination of crystalline phases forming hydrides under the conditions applied, and reduced particle size.

Acknowledgements: *The authors would like to thank the European regional development fund within the Operational Programme "Science and Education for Smart Growth" under the project CoC Hitmobil BG05M2OP001-0014-C01. Research equipment of the Distributed Research Infrastructure INFRAMAT D01-306/20.12.2021, part of the Bulgarian National Roadmap for Research Infrastructures, supported by the Bulgarian Ministry of Education and Science was used in this investigation.*

REFERENCES

1. V. A. Yartys, M. V. Lototskyy, E. Akiba, R. Albert, V. E. Antonov, J. R. Ares, M. Baricco, N. Bourgeois, C. E. Buckley, J. M. von Colbe Bellosta, J.-C. Crivello, F. Cuevas, R. V. Denys, M. Dornheim, M. Felderhoff, D. M. Grant, B. C. Hauback, T. D. Humphries, I. Jacob, T. R. Jensen, P. E. de Jongh, J.-M. Joubert, M. A. Kuzovnikov, M. Latroche, M. Paskeviciusi, L. Pasquini, L. Popilevsky, V. M. Skripnyuk, E. Rabkin, M. V. Sofianos, A. Stuart, G. Walker, H. Wang, C. J. Webb, M. Zhu, *Int. J. Hydrog. Energy,* **44**, 7809 (2019).
2. Z. Gavra, G. Kimmel, Y. Gefen, M. H. Mintz, *J. Appl. Phys.*, **57**, 4548 (1985).
3. E. Rönnebro, D. Noréus, *Appl. Surf. Sci.,* **228**, 115 (2004).
4. L. Li, T. Akiyama, J. Yagi, *Int. J. Hydrog. Energy,* **26**, 1035 (2001).
5. J. Cermak, B. David, *Int. J. Hydrog. Energy*, **36**, 13614 (2011).
6. J. Cermak, K. Kral, *J. Alloys Compds.,* **546**, 129 (2013).
7. S. Orimo, K. Ikeda, H. Fujii, Y. Fujikawa, Y. Kitano, K. Yamamoto, *Acta Mater.*, **45**, 2271 (1997).
8. R. A. Varin, T. Czujko, J. Mizera, *J. Alloys Compds.*, **354**, 281 (2003).
9. R. A. Varin, T. Czujko, *Mater. Manuf. Process*, **17**, 129 (2002).
10. P. Tessier, H. Enoki, M. Bououdina, E. Akiba, *J. Alloys Compds.*, **268**, 285 (1998).
11. F. C. Gennari, M. R. Esquivel, *J. Alloys Compds.*, **459**, 425 (2008).
12. M. Polanski, T. K. Nielsen, I. Kunce, M. Norek, T. Płociński, L. R. Jaroszewicz, C. Gundlach, T. R. Jensen, J. Bystrzycki, *Int. J. Hydrog. Energy*, **38**, 4003 (2013).
13. R. Martínez-Coronado, M. Retuerto, B. Torres, M. J. Martínez-Lope, M. T. Fernández-Díaz, J. A. Alonso, *J. Hydrog. Energy*, **38**, 5738 (2013).
14. X. Hou, R. Hu, T. Zhang, H. Kou, W. Song, J. Li, *Int. J. Hydrog. Energy*, **39**, 19672 (2014).
15. A. Baran, M. Polański, *Materials*, **13**, 1936 (2020).
16. X. Q. Tran, S. D. McDonald, Q. Gu, T. Yamamoto, K. Shigematsu, K. Aso, E. Tanaka, S. Matsumura, K. Nogita, *J. Power Sources*, **341**, 130 (2017).
17. Y. Fu, Z. Ding, S. Ren, X. Li, S. Zhou, L. Zhang, W. Wang, L. Wu, Y. Li, S. Han, *Int. J. Hydrog. Energy*, **45**, 28154 (2020).
18. Y. Liu, D. Chabane, O. Elkedim, *Energies*, **14**, 5758 (2021).
19. N. Cui, B. Luan, H. K. Liu, H. J. Zhao, S. X. Dou, *J. Power Sources*, **55**, 263 (1995).
20. N. Cui, P. He, J. L. Luo, *Acta Mater.*, **47**, 3737 (1999).
21. N. Cui, J. L. Luo, *Electrochimica Acta*, **45**, 3973 (2000).
22. Y.-H. Zhang, D.-L. Zhao, B.-W Li, H.-P. Ren, Sh.-H. Guo, X.-L. Wang, *J. Alloys Compds.*, **491**, 589 (2010).
23. X. Hou, R. Hu, T. Zhang, H. Kou, W. Song, J. Li, *Mater. Charact.*, **106**, 163 (2015).
24. H. Shao, X. Li, *J. Alloys Compd.*, **667**, 191 (2016).
25. M. V. Simičić, M. Zdujić, R. Dimitrijević, Lj. Nikolić-Bujanović, N. H. Popović, *J. Power Sources*, **158**, 730 (2006).
26. E. Grigorova, P. Tzvetkov, S. Todorova, P. Markov, T. Spassov, *Materials*, **14**, 1936 (2021).
27. Eva Software Bruker. Available online: https://www.bruker.com/products/x-ray-diffraction-and-elemental-analysis/x-ray-diffraction/xrd-software/eva.html.
28. G. Zheng, B. N. Popov, R. E. White, *J. Electrochem. Soc.*, **143**, 834 (1996).
29. O. Reiko, L. Chao-Ho, H. Chii-Shyang, *J. Alloys Compds.*, **580**, S368 (2013).
30. N. Cui, J. L. Luo, K. T. Chuang, *J. Electroanal. Chem.*, **503**, 92 (2001).
31. Y.-H. Zhang, K. Lü, D.-H. Zhao, Sh.-H. Guo, Y. Qi, X.-L.Wang, *Trans. Nonferrous Met. Soc. China*, **21**, 502 (2011).
32. N. Cui, J. L. Luo, *Int. J. Hydrog. Energy*, **24**, 37 (1999).